

Fast development of purple nonsulfur bacteria (PNSB) in a bubble column photobioreactor: influence of carbon source and dissolved O₂ availability on wastewater treatment performance

Tengge Zhang^{a,b}, Guillermo Quijano^{a*}, Meng Wang^{b*}

- a. Laboratory for Research on Advanced Process for Water Treatment, Instituto de Ingeniería, Unidad Académica Juriquilla, Universidad Nacional Autónoma de México, Blvd. Juriquilla 3001, Querétaro 76230, Mexico
- b. Department of Energy and Mineral Engineering, Pennsylvania State University, University Park, PA, 16802, USA

*Corresponding authors:

Tel: +52-55-4779-7128. Email: gquijano@nextgenbiotech.us (Guillermo Quijano)

Tel: +1-814-863-6388. Email: mxw1118@psu.edu (Meng Wang)

14 **Abstract**

15 Photobioreactors with purple nonsulfur bacteria (PNSB) constitute a
16 promising technology for wastewater treatment, gas purification, and high value-
17 added bioproducts. In this work, different operational strategies were tested to
18 investigate their impacts on photobioreactor performance, biomass properties, and
19 microbial community. It showed that the operational conditions significantly
20 influence the performance and microbial composition of PNSB photobioreactors.
21 Anaerobic conditions favored the dominance of *Rhodopseudomonas* spp. and
22 moderate COD removal efficiency (36.7%), while aerobic conditions significantly
23 enhanced COD removal efficiency (91.7%) but altered the microbial community
24 composition from PNSB to aerobic heterotrophic microorganisms, such as *Delftia* sp.
25 and *Microbacterium* sp.. The removal ratio of chemical oxygen demand (COD):N:P
26 was 100:10:2 under anaerobic conditions with continuous CO₂ supply, while it was
27 100:1:1 under aerobic conditions with continuous supply of a CO₂/O₂ mixture. Net
28 CO₂ removal efficiencies of 2.8% and 5.4% were recorded under anaerobic conditions
29 with and without the addition of organic carbon, respectively. The outlet CO₂
30 concentration showed that CO₂ uptake occurred under dark and anaerobic conditions
31 without organic carbon. The reduced production of extracellular polymeric substances
32 (EPS) was observed after COD was removed from the influent, preventing granule
33 formation.

34

35 **Keywords:** Anaerobic condition, CO₂ uptake, COD removal, Microbial community,
36 Wastewater treatment.

37

38 **1. Introduction**

39 The global rise in wastewater production and the environmental challenges
40 associated with its management require sustainable and effective treatment methods.
41 Traditional physio-chemical treatment processes, although effective, often come with
42 high operational costs, chemical usage, and secondary pollution [1, 2]. Purple
43 nonsulfur bacteria (PNSB) offer a biological alternative that could address some of
44 these challenges, due to their versatile metabolic capabilities and ability to thrive in
45 various environmental conditions [3].

46 PNSB have been applied in photobioreactors for wastewater treatment and gas
47 purifying by their ability to thrive in anaerobic conditions and utilize a wide range of
48 carbon sources and nutrients, which will be converted into bioenergy and useful
49 bioresources [4-6]. A complex interaction of metabolisms can be deployed by PNSB,
50 including photoheterotroph, photoautotroph, respiration, fermentation, and nitrogen
51 fixation, depending on light/dark conditions, carbon source, and O₂ availability [7]. In
52 aerobic conditions, PNSB can grow by respiration, while in anaerobic conditions with
53 light, they grow as photoautotrophs with CO₂ as the sole carbon source or grow as
54 photoheterotrophs with organic carbon sources, such as organic acids, sugars, and
55 volatile fatty acids. Various configurations of PNSB photobioreactors were applied
56 and evaluated, including batch reactor and continuous column reactor [6], to treat
57 municipal wastewater, soybean wastewater, agricultural wastewater, etc. Most of
58 PNSB wastewater treatment systems were reported with a strong ability on chemical
59 oxygen demand (COD) removal, with over 70% removal efficiency [8, 9]. Previous
60 research showed that in anaerobic membrane bioreactors (AnMBR) treating domestic
61 wastewater, total N and total P removal efficiencies could reach up to 92% and 98%,
62 respectively [10].

63 However, in natural environments, PNSB always coexist with various
64 microorganisms. Compared with other bacteria, PNSB have a lower growth rate [11].
65 The slow growth rate makes it challenging for PNSB to outcompete with other
66 microorganisms for nutrients and spaces, preventing its enrichment from the initial
67 inoculum containing a mixed microbial community. PNSB can assimilate carbon (C),
68 nitrogen (N), and phosphorus (P) from wastewater with the COD:N:P ratio of
69 100:6.4:1.1 [12]. Due to the complicated factors and requirements, the bubble column
70 photobioreactor is a promising system for the efficient cultivation of PNSB due to its
71 high mass transfer rate and, uniform mixing, and adjustable light and gas availability
72 [13].

73 It was reported that *Rhodobacter* could be enriched under high acetate
74 concentrations (5-20 mmol/L), while *Rhodopseudomonas* was enriched at lower
75 concentrations (0.5-1 mmol/L) [14]. The optimum temperature of PNSB was 25 °C-
76 30 °C [15]. The pH of 7-8 was preferred for PNSB growth. The highest organic
77 carbon removal and lowest inorganic carbon removal were observed at pH 8.0, while
78 pH 5.0 showed the highest inorganic carbon removal [16]. In addition, the highest
79 maximum specific growth rate of *Rhodopseudomonas palustris* was achieved at a light
80 intensity of around 1800 $\mu\text{mol}/\text{m}^2/\text{s}$ [17]. PNSB granules were successfully enriched
81 out of activated sludge in a sequencing batch reactor (SBR) with acetate-based
82 synthetic water and achieved promising COD and nutrient removal efficiencies of
83 95% and over 70%, respectively [18]. However, it took five months to inoculate the
84 biomass in batch mode before switching to SBR mode. Most other studies focusing on
85 reactor performance, bioproducts, or growth kinetics of PNSB, used enriched PNSB
86 culture instead of mixed inoculum, which was easier to gain [19, 20]. Therefore,
87 methods for the fast enrichment of PNSB to promote the development of PNSB

88 applications are needed.

89 Moreover, PNSB granules are desired to facilitate biomass harvesting due to
90 their enhanced settling ability. Biomass granulation can also improve the reactor
91 performance by increasing the solid retention time (SRT), resistance to environmental
92 stresses, and microbial activity. Aeration plays a vital role in the biomass granulation
93 process to maintain the microbial structure and the metabolism pathways. Prior
94 research showed that high air velocity can provide shear force to stimulate the
95 production of extracellular polymeric substances (EPS), which are critical for the
96 formation and maintenance of granules [21, 22]. In contrast, *Rb. capsulatus* might
97 produce a heat-labile metabolites inducing disaggregation. Higher COD/N
98 ratios could also lead to disaggregation because of the overgrowth of filamentous
99 bacteria [23].

100 This study aimed to approach strategies for the fast development of PNSB in a
101 simple bioreactor configuration. For this purpose, a bubble column photobioreactor
102 that was continuously supplied with different ratios of CO₂ and O₂ was implemented.
103 The reactor was inoculated with activated sludge due to its wide availability in bulk
104 amounts. Different operational strategies were applied to investigate their impacts on
105 the reactor performance (COD, nitrogen and phosphorous removal), biomass
106 properties (chlorophyll, carotenoids, and exopolysaccharide content), and the resulting
107 microbial community.

108

109 **2. Materials and methods**

110 **2.1. Synthetic wastewater and inoculum**

111 Medium-strength synthetic wastewater with a COD of 475.5±10.4 mg/L
112 modified according to García et al. was fed to the reactor [24]. NaHCO₃ and CaCl₂ at

113 3 and 0.005 g/L, respectively were added to keep the pH above 7 and to promote
114 biomass granulation. The composition of the medium-strength synthetic wastewater
115 was (g/L): CH₃COONa (0.6), NH₄Cl (0.31), K₂HPO₄ (0.073), NaHCO₃ (3), and CaCl₂
116 (0.005). In addition, 10 mL trace element stock solution was added to 1 L of media
117 with the following composition (g/L): EDTA-C₁₀H₁₆N₂O₈ (0.5), FeSO₄·7H₂O (0.2),
118 ZnSO₄·7H₂O (0.01), MnCl₂·4H₂O (0.003), H₃BO₃ (0.03), CoCl₂ (0.011), CuCl₂·2H₂O
119 (0.162), NiCl₂·6H₂O (0.002), NaMoO₄·2H₂O (0.003), and MgSO₄·7H₂O (0.02).
120 Secondary activated sludge from a wastewater treatment plant performing
121 nitrification-denitrification was used as the inoculum (Querétaro, Mexico). The
122 reactor was inoculated with 10% (v/v) activated sludge relative to the working volume
123 of the reactor (3.6 L), reaching an initial total suspended solids (TSS) concentration of
124 0.32 g TSS/L.

125 **2.2. Reactor setup and operation**

126 As shown in Figure 1, a laboratory-scale cylindrical column (62.5 cm height,
127 8.7 cm inner diameter, total volume of 3.7 L) was operated at a working volume of
128 3.6 L. Magnetic stirring (150 rpm) was provided at the bottom to keep the biomass
129 suspension. The reactor was operated with 12/12 h light/dark photoperiods at room
130 temperature (Figure. 1). An average light intensity of ~200 µmol/m²/s was provided
131 by a dual strip LED light (Model MNSL, Lithonia Lighting, Mexico), which was
132 measured inside the reactor at the bottom, middle and top of the column. The 12/12 h
133 photoperiod was controlled by a digital control unit connected to a Lab-Quest data
134 acquisition card (Venier, Beaverton, OR, USA). To control the concentration of CO₂
135 flowing into the reactor, CO₂ and air or O₂ were supplied at desired flow rates via
136 mass flow controllers (Model GFC, Aalborg Instruments, New York, USA) and
137 mixed in a gas chamber before entering the column. The mixed gas was introduced to

138 the bottom of the column by a stone diffuser at a total flow rate of 0.2 L/min. A settler
139 of 0.9 L was implemented to avoid biomass washing out in the column. Since the CO₂
140 supply could lead to acidification of the culture medium, which was detrimental to the
141 cultivated organisms, 3 g/L of NaHCO₃ was added to the influent to keep the pH
142 above 7. The column was equipped with dissolved oxygen (DO), pH, and temperature
143 sensors, as well as a gas sensor to monitor the CO₂ concentration at the gas outlet.
144 DO, pH, temperature and CO₂ concentration data were acquired every hour
145 throughout the experiment.

146 The liquid phase of the photobioreactor was operated in batch mode for 11
147 days, while the gas phase was supplied continuously at a gas retention time (GRT) of
148 18 min, determined as follows:

$$149 \quad GRT = V/F \quad (1)$$

150 where V and F stand for the working volume of the reactor and the gas flow rate,
151 respectively. Thereafter, the reactor was also operated in continuous mode. For this
152 purpose, the liquid influent, effluent, and biomass recirculation were controlled by
153 three automated peristaltic pumps (model 77200-50, Cole-Parmer, USA), with flow
154 rates of 1, 2, and 1 mL/min, respectively, resulting in a hydraulic retention time
155 (HRT) of 2.5 days. Table 1 summarizes the COD concentrations in wastewater and
156 gas compositions tested. In phase I, II, and III, a mixture of CO₂ and N₂ was supplied
157 to keep the reactor in anaerobic condition, while in phase IV, a mixture of CO₂ and air
158 was supplied to keep the reactor in aerobic condition. A DO sensor was used to
159 monitor the anaerobic/aerobic condition throughout the experiment. In phase III, COD
160 in the form of acetate was not supplied to evaluate the impact of carbon source on the
161 metabolism pathways of the microorganisms.

162 **2.3. Molecular biology analysis**

163 Mixed liquor samples (50 mL) from the reactor were periodically drawn on
164 days 0, 28, 41, and 57, and stored at -20°C for microbial analysis.
165 Genomic DNA was extracted with PowerSoil[®] DNA isolation kit (MOBIO, USA).
166 The extracted DNA samples were submitted to the Research and Testing Laboratory
167 (RTL, Lubbock, USA) for Illumina MiSeq sequencing analysis of microalgal (18S
168 rRNA, primers: EukA7F 5'-AACCTGGTTGATCCTGCCAGT-3', EUK555R 5'-
169 GCTGCTGGCACCAAGACT-3') and bacterial cells (16S rRNA, primers: 28F 5'-
170 GAGTTGATCNTGGCTCAG-3', 388R 5'-TGCTGCCTCCGTAGGAGT-3') [25].
171 The resultant sequences were processed utilizing DADA2 v1.26 within the R
172 environment. Forward and reverse reads were filtered and truncated to 200 and 250
173 nucleotides, respectively, chimera sequences were removed, and an amplified
174 sequence variant table was obtained. Taxonomic classifications were assigned to
175 representative sequences through the application of a Naïve Bayesian classifier, and
176 two different dataset references, SILVA 132 and PR2 5.0, were used for 16S and
177 18S, respectively [26].

178 **2.4. Analytical methods**

179 The liquid samples were filtered through 0.22 μm nylon membranes before the
180 chemical analysis. The soluble COD and NH_4^+ concentrations were determined by
181 USEPA reactor digestion method (Hach 8000) and salicylate method (Hach 10031)
182 respectively. Concentrations of NO_2^- , NO_3^- , and PO_4^{3-} were measured by ion
183 chromatography (IC) system (model ICS 1500, Dionex, Sunnyvale, CA, USA). TSS
184 and volatile suspended solids (VSS) were determined according to Standard Methods
185 [27].

186 Chlorophyll and carotenoids were determined according to Osório et al. with
187 100% methanol [28]. Briefly, 10 mL mixed liquor was centrifuged at 2500 rpm for 10

188 min. The supernatant was discarded and 100% methanol was added to the final
189 volume of 10 mL. The mixture was resuspended by a vortex. For sufficient extraction,
190 the mixture was kept at 4 °C in dark for over 12 h. Then, the mixture was centrifuged
191 at 2500 rpm for 10 min to obtain a clear supernatant. The absorbance of the
192 supernatant was measured in a 1-cm cuvette at the wavelengths of 480 nm, 632 nm,
193 652 nm, 665 nm, 696 nm, and 750 nm in duplicate by a spectrophotometer (model
194 VE-5600UV, Velab). The calculations of chlorophyll a, chlorophyll b, chlorophyll c,
195 chlorophyll d, and carotenoids concentrations can be found in Osório et al 2020 [28].

196 EPS was extracted by a modified heating method [29]. Briefly, 10mL mixed
197 liquor sample was centrifuged at 5000g for 15 min. The supernatant was filtered
198 through 0.22 µm nylon membrane, and the filtrate was collected to represent the
199 loosely bound EPS (LB-EPS) fraction. The supernatant was discarded, and the
200 residual biomass was resuspended with 0.9% (w/v) NaCl solution to the original
201 volume (10 mL). The mixture was heated at 70 °C for 30 min. The extracted solution
202 was centrifuged at 10,000g for 20 min under 4 °C, and the supernatant was filtered
203 through 0.22 µm nylon membrane. The filtrate was collected to represent the tightly
204 bound EPS (TB-EPS) fraction. The EPS samples are stored at –20 °C prior to
205 analysis. Extracellular polysaccharides (PS) and proteins (PN) are measured by the
206 colorimetric method and the Lowry-Folin method, respectively [30, 31].

207

208 **3. Results and discussion**

209 **3.1. COD and nutrients removal performance**

210 COD removal performance is shown in Figure 2a. During batch operation in
211 the experimental phase I, with continuous CO₂ and N₂ supply, the COD concentration
212 was reduced from 551.5 mg/L to 353.5 mg/L within 11 days (corresponding to a
213 removal efficiency of 35.9%). During phase II, under HRT of 2.5 days and continuous

214 supply of CO₂ and N₂ gas, the COD removal was stable with an average removal
215 efficiency of 36.7%, corresponding to an average removal rate of 68.8 g COD/m³·d
216 (Table 2). In the experimental phase II, CO₂ and N₂ were continuously supplied,
217 which stripped the O₂ potentially produced via photosynthesis. Since no DO was
218 available (Figure. 2C), COD removal was attributed to photoheterotrophic metabolism
219 during the light period and respiration during dark period (Figure 3). A clear increase
220 of biomass concentration (TSS) in the photobioreactor was observed, passing from 0.5
221 g/L at the end of experimental phase I to 0.7 mg/L at the end of experimental phase II.
222 An average biomass specific growth rate of 0.10/day was recorded under the
223 experimental conditions set in experimental phase II (Table 2).

224 Previous research showed that when using purple phototrophic bioreactors to
225 treat raw domestic wastewater in membrane systems, above 90% COD removal was
226 achieved [12]. In those cases, the soluble COD concentrations of the influent were
227 245 mg/L and 138 mg/L, respectively, which were much lower than that of this
228 research. A recent study using purple phototropic bacteria in an anaerobic membrane
229 bioreactor (PAnMBR) for refinery water treatment achieved a maximum soluble COD
230 removal of 75% [32]. COD/Biomass ratio in this study was 0.8 g COD/g VSS, which
231 was lower than most prior studies (1-4 g COD/g VSS) which showed over 50%
232 removal of COD with HRT of 1.5-4 days [4, 33, 34]. The COD:N:P removal ratio in
233 this study was consistent with previous research on PNSB (will be discussed later in
234 this section), indicating that the main metabolisms during the process were acted by
235 PNSB in this study. However, in other studies, the bioreactors were operated longer
236 than this study, which ensured that the biomass adjusted well to the environment.
237 Note that the reactor in this study was seeded with activated sludge. The shift of
238 microbial community resulting from different operational conditions can cause

239 different COD removal performances.

240 In order to compare the impact of carbon source on the reactor performance,
241 organic carbon source was eliminated during the experimental phase III, and the COD
242 concentration was progressively decreased from 223 mg/L to 42.5 mg/L in the
243 effluent. The higher COD values recorded in the first days of experimental phase III
244 were probably attributed to the biomass decay and the carryover of COD from phase
245 II (Figure 2b). Sudden changes in COD have may trigger biomass decay in
246 photobioreactors [24]. The SRT of the system was 6.4 days. It is expected to take
247 around 10 days to decay more than half of biomass.

248 During phase IV, a mixture of air and CO₂ was fed to the reactor continuously,
249 while organic carbon was reinstated in the influent. A COD removal efficiency of up
250 to 91.7% was achieved in phase IV due to the presence of O₂ in the system. This
251 oxygen promoted the proliferation of aerobic heterotrophic microorganisms that use
252 organic matter as carbon and energy sources, and employ more efficient metabolism
253 pathways to break down organic compounds. This results in a higher COD removal
254 efficiency compared to anaerobic conditions. An average removal rate of 175.8 g
255 COD/m³·d and an average specific COD removal rate of 311.8 g COD/kg VSS·d
256 indicated that the reactor reached a high COD removal performance with the presence
257 of O₂. The presence of O₂ promoted the respiration of heterotrophs, which used COD
258 as the carbon source. In the algal photobioreactor with intermittent illumination, COD
259 removal could reach around 70% [35], which was lower than the photobioreactor in
260 this study. As it will be discussed in detail in Section 3.5, changes in COD and O₂
261 availability indeed produced profound changes in the predominant microbial
262 communities in each experimental phase tested.

263 The experimental conditions in experimental phases II and IV allowed for

264 COD removal in the photobioreactor with the best performance observed in phase IV
265 due to O₂ availability, which promoted the heterotrophic metabolism. If a CO₂-rich
266 gas stream is intended for use as an inorganic carbon source in photobioreactors for
267 wastewater treatment, it is recommended to mix this stream with air to ensure an
268 adequate supply of O₂ and facilitate high COD removal. Additionally, the conditions
269 established during experimental phase II also accomplished the removal of organic
270 matter at a rate of 68.8 g/m³·d. Moreover, switching to aerobic conditions (as in phase
271 IV) for a brief period can be used as a polishing strategy for COD removal if required.

272 As for the nutrient removal, NH₄⁺-N was reduced from 72.3 mg/L to 43.6
273 mg/L, and PO₄³⁻-P was reduced from 20.9 mg/L to 11.5 mg/L for the batch operation
274 of the reactor with during phase I (Figure 3). The removal ratio of COD:N:P was
275 100:15:5. During phase II, the removal efficiencies of NH₄⁺-N and PO₄³⁻-P were
276 26.6% and 11.9%, respectively. The removal ratio of COD:N:P was 100:10:2, which
277 was consistent with previous research on purple bacteria in photo anaerobic
278 membrane bioreactor (100:6.4:1.1) [12]. Since the uptake of PO₄³⁻-P by purple
279 bacteria under anaerobic condition was lower than that under aerobic condition and
280 the uptake of PO₄³⁻-P by phosphate-accumulating organisms (PAOs) required both
281 anaerobic and aerobic conditions. While only anaerobic condition was provided
282 during phase II, a limited PO₄³⁻-P removal efficiency was observed.

283 During phase III, the average NH₄⁺-N removal performance was similar to
284 phase II. The PO₄³⁻-P average removal efficiency improved to 27.1% due to the
285 growth of biomass (VSS) compared with phase II, since the average specific removal
286 rate did not improve.

287 During phase IV, the NH₄⁺-N removal decreased, with an average removal
288 efficiency of 10.0%. The removal ratio of COD:N:P was 100:1:1. The PO₄³⁻-P

289 removal performance increased because O₂ in the gas inlet provided an aerobic
290 condition, and anaerobic condition was provided inside the biomass granular. So that
291 the two processes (P release and P accumulation) for PO₄³⁻-P removal can be
292 completed.

293 Previous research showed that in a continuous PNSB photobioreactor, NH₄⁺-N
294 and PO₄³⁻-P removal rates reached up to 113 g N/m³·d and 15 g P/m³·d, respectively
295 [18]. In other studies with PNSB wastewater treatment, the removal efficiencies of
296 NH₄⁺-N and PO₄³⁻-P were more than 60% and 55%, respectively [8, 34, 36]. These
297 were much higher than the results in this study. However, the previous research
298 applied a higher SRT (11 days) and a higher biomass concentration of up to 4 g
299 VSS/L, over 4 times more than this study [18].

300 **3.2. CO₂ uptake and the impact of carbon source**

301 The average CO₂ removal efficiency was 2.8% in phase II (Figure 4a). The
302 average removal efficiency of CO₂ increased to 5.4% in phase III. The CO₂ removal
303 rates in phases II and III were 0.11g/(L day) and 0.22 g /(L day), respectively. CO₂
304 was the only carbon source of the reactor in phase III, and purple bacteria could
305 utilize CO₂ for photosynthesis when there was no other carbon source or oxygen.
306 During phase IV, there was almost no CO₂ removal from the system, due to the
307 aerobic respiration of bacteria with the presence of organic carbon. O₂ and organic
308 carbon were used by biomass in the reactor, including purple bacteria for aerobic
309 respiration and CO₂ was generated as a byproduct. In general, the conditions tested in
310 this study did not support effective CO₂ removal in the photobioreactor. However, the
311 outlet CO₂ concentration had a periodical change within each operation cycle (1 day),
312 where there were obvious peak in the light phase and valley values in the dark phase
313 during each day (Figure. 4b). It meant negativa removal of CO₂ with light and

314 positive removal of CO₂ in dark. Therefore, for practical applications, a potential
315 strategy is to intermittently introduce CO₂ during the dark phase to prevent negative
316 removal during the light phase. This approach optimizes the gas purification
317 performance, carbon utilization, and energy costs associated with the gas supply for
318 the system.

319 Under anaerobic conditions with light, purple bacteria can utilize CO₂ as a
320 carbon source for photosynthesis in the absence of organic carbon. During phase III,
321 with CO₂ being the sole carbon source for photosynthesis, PNSB was able to consume
322 more CO₂. This led to an improvement in CO₂ removal efficiency, which was nearly
323 double that of phase II. Moreover, when both organic carbon and CO₂ are present, the
324 bacteria prioritize using organic carbon as their primary carbon source. However, in
325 the presence of O₂, purple bacteria will undergo aerobic respiration rather than
326 photosynthesis, consuming organic carbon instead of CO₂.

327 Meanwhile, in aerobic conditions, heterotrophic bacteria will also perform
328 respiration and produce CO₂. Therefore, CO₂ removal efficiency in photobioreactors
329 depends on their consumption by photosynthesis and their production by respiration.
330 In an anaerobic/aerobic photobioreactor treating textile wastewater, a negative
331 removal efficiency of inorganic carbon was reported for the entire experimental
332 period due to the CO₂ produced from the anaerobic degradation of the organic matter.
333 The CO₂ produced was consumed in the following aerobic photobioreactor by algae
334 [37], while positive CO₂ production was observed during the anaerobic phase. It
335 showed that the highest inorganic carbon removal efficiency was observed at pH 5.0,
336 while the lowest removal efficiency was found at pH 8.0 because of the bicarbonate
337 degradation at the lower pH [16]. This might be one of the reasons for the low CO₂
338 removal in this study. The CO₂ fixation rate was reported in the range of 0.1-1.5

339 g/Lday in photobioreactors with different illumination durations each day [38-40]. A
340 prior study demonstrated that CO₂ removal rate by PNSB was 0.56 g/(L· day) with
341 12h-12h light-dark cycle [38], which is significantly higher than the rates observed in
342 this study. However, the biomass concentration in that study was 2 g/L, considerably
343 higher than this study (< 1 g/L). The lower biomass concentration in the reactor
344 resulted in low CO₂ removal efficiency. Moreover, their calculations of CO₂ fixation
345 rate were based on the production of biomass instead of the CO₂ removal in gas phase,
346 and organic carbon uptake was not counted. This study presented a direct
347 measurement of CO₂ removal based on the change of CO₂ concentration in gas phase.

348 **3.3. Biomass properties**

349 It showed that the biomass had a high chlorophyll b content and a small
350 carotenoid content, which are the main pigments of purple bacteria (Figure. 5a). For
351 some algal species, the content of chlorophyll a is higher than chlorophyll b (which
352 would be explained in Section 3.5) [41], so the low chlorophyll a content indicated
353 that algae was not dominant in the reactor. Since the values of cholorophyll a, c, and d
354 were close to 0, the total chlorophyll was mainly contributed by chlorophyll b. The
355 total chlorophyll content increased from 2 mg/g VSS to 14 mg/g VSS during phase II
356 and phase III due to the benefit of anaerobic conditions for purple bacteria. It
357 decreased significantly to the initial value (2 mg/g VSS) in phase IV because the
358 aerobic condition promoted the growth of other bacteria. The pigment contents
359 revealed the switch of microbial community composition, indicating that anaerobic
360 conditions could promote the growth of purple bacteria by reducing competition with
361 other microorganisms.

362 Prior research has shown that EPS played an important role in the formation
363 and maintenance of granules derived from activated sludge granular (AGS). EPS can

364 increase the hydrophobicity of the cells' surface, and increasing the ratio of protein to
365 polysaccharide can reduce the negative surface charge of cells, resulting in the
366 decrease of their electrostatic repulsion. The changes of hydrophobicity and surface
367 charge can promote the granulation process [42]. EPS could also protect biomass from
368 harsh conditions such as extreme temperatures, pH fluctuations, and toxic substances
369 [43]. However, high EPS production may reduce microbial growth rates, as more
370 energy is expended in synthesizing EPS rather than biomass [44]. Excessive EPS can
371 also cause clogging in the bioreactor, hinder mass transfer, and increase operational
372 costs due to more frequent cleaning and maintenance requirements [45]. The initial
373 sludge had the highest EPS content (Figure 5b). It decreased rapidly because of
374 limited COD in batch mode throughout the time. In phase II, the biomass had a higher
375 EPS content during the first week (day 18) and decreased later. The EPS content
376 remained consistent with the end of phase II throughout phase III. In contrast, the
377 chlorophyll content peaked during this phase, indicating the highest distribution of
378 purple bacteria in the biomass. With organic carbon and O₂ provided in phase IV, EPS
379 production and PN/PS ratio increased, indicating an appropriate granular formation
380 condition. The initial activated sludge and the biomass in phase IV had higher EPS
381 contents, consistent with that aerobic condition and organic carbon can promote EPS
382 production. However, during the experiment, no mature granules were observed. The
383 reactor was operated under a continuous flow mode, lacking settling time and
384 selection pressure that promotes granule formation. In phase III, the limited organic
385 carbon source led to a decrease in EPS production, which prevented the further
386 granulation process. Besides, the lack of filamentous microorganisms might be
387 another reason for the lack of mature granules. Although the system produced more
388 EPS than conventional activated sludge system [46, 47], indicating the potential for

389 granule formation, it still produced much less EPS than other PNSB granule systems
390 (over 200 g EPS/g VSS) operated more than 200 days [48]. The short duration of
391 anaerobic phase with organic carbon in this study might be another factor causing the
392 low EPS production and lack of granular formation.

393 The changes in COD and O₂ availability induced changes in the microbial
394 communities, which could be observed via drastic color changes in each experimental
395 phase (Figure. 6). In phase II, the color changed from yellow to brown, kept in brown
396 during the whole phase III, and became much lighter at the end of phase IV,
397 indicating that purple bacteria were the dominant taxa in phases II and III and decayed
398 in phase IV, which can be confirmed by microbial analysis in section 3.5.

399 **3.4. Microbial community characterization**

400 16S rRNA analysis indicated that there was almost no overlap between the
401 dominant species of sludge used as inoculum and in the later phases (Figure 7a). The
402 most dominant species in the sludge inoculum were *Candidatus Competibacter sp.*
403 and *Caldilinea sp.*, with relative abundances of 9.2% and 9.0%, respectively. In phase
404 II and phase III in anaerobic conditions, *Rhodopseudomonas* spp., a PNSB, became
405 the dominant species with relative abundances of 92.8% and 94.6%, respectively. The
406 relative abundances of the second dominant species, *Thiobaca sp.*, which is a purple
407 sulfur bacterium (PSB), were 2.6% and 1.2%, respectively. The relative abundances
408 of *Thiobaca sp.* were much lower than *Rhodopseudomonas* spp. since there was
409 limited sulfur source. In phase IV with aerobic condition, the relative abundance of
410 *Rhodopseudomonas* spp. decreased to 36.6%. *Delftia sp.* and *Microbacterium sp.*
411 became the other two dominant species with relative abundances of 18.5% and 13.6%,
412 respectively, which contributed to the organic matter removal and nitrogen removal
413 [49, 50]. The aerobic condition did not help the recovery of microorganisms to the

414 initial composition but helped develop some aerobic bacteria species. 18S rRNA
415 analysis showed the relative abundances of algae species (Figure 7b). It showed
416 almost no algae in the sludge used as inoculum (0.13%). In phase II and phase III,
417 algae became the dominant Eukaryote. The relative abundances of *Chlorella*
418 *sorokiniana*, which was the main algae species, were 84.5% and 75.6%, respectively,
419 while it dropped to 6.2% in phase IV. The main pigment of *Chlorella sorokiniana* was
420 chlorophyll a [51]. As it was mentioned in Section 3.4, there was almost no
421 chlorophyll a content in the biomass. Thus, PNSB was the main dominant taxa in the
422 reactor instead of algae.

423 *Rhodopseudomonas* spp. could perform photosynthesis under anaerobic
424 conditions with light and various carbon sources, while most other microorganisms
425 require O₂ and organic carbon to grow, which allowed *Rhodopseudomonas* spp. to
426 outcompete with other microorganisms and became the dominant species. Since
427 *Rhodopseudomonas* spp. can fix nitrogen, conversing N₂ to NH₄⁺ under anaerobic
428 conditions [52], which might be the reason for the low NH₄⁺ removal during the
429 experiment. Under aerobic conditions, PNSB are unable to grow through the
430 photosynthetic process [53, 54], leading to a general decline in biomass
431 concentrations, (Figure. 2b) and the decrease of relative abundance of
432 *Rhodopseudomonas* spp.. The photobioreactor with PNSB could perform different
433 metabolic pathways depending on light availability and the presence of CO₂ and O₂
434 (Table 3). In anaerobic conditions with light and the existence of both CO₂ and O₂
435 organic carbon source (acetate acid), PNSB prefers to use organic carbon as the
436 carbon source and grows photoheterotrophically. When CO₂ is the sole carbon source,
437 PNSB undergoes the photoautotrophic pathway. While under aerobic conditions,
438 PNSB can consume organic carbon by respiration, and CO₂ will not be consumed.

439 However, their growth rate under aerobic conditions was significantly lower than
440 under anaerobic conditions [53], which is consistent with this study. This slower
441 growth also stemmed from the competition between PNSB and other heterotrophs,
442 such as *Delftia sp.* and *Microbacterium sp.*, which were better adapted to cope with
443 oxidative stress, giving them a survival advantage under high oxygen conditions. Fig.
444 8 shows the metabolic pathways of COD removal PNSB under different aeration and
445 light conditions. Aerobic respiration is the main catabolic pathway for organic matter
446 degradation under aerobic conditions, involving three key steps: glycolysis (EMP) or
447 Entner–Doudoroff (ED) pathway, the tricarboxylic acid (TCA) cycle, and the electron
448 transport chain. Under light-anaerobic conditions, energy is generated through
449 photophosphorylation as the main process and substrate-level phosphorylation. The
450 primary catabolic pathways for organic carbon degradation are the EMP/ED pathway,
451 followed by fermentation [55].

452

453 **4. Conclusions**

454 This work confirmed that PNSB can be quickly enriched under anaerobic
455 conditions and the continuous supply of CO₂. PNSB became predominant within 28
456 days of operation, even under a light intensity of 200 μmol/m²/s. *Rhodopseudomonas*
457 spp. was the dominant PNSB species, with a relative abundance of over 90%. The
458 photobioreactor achieved a removal ratio of COD:N:P of 100:10:2 when no O₂ was
459 supplied. However, when 20.4% O₂ was provided, the removal ratio of COD:N:P was
460 100:1:1, which highlighted the relevance of the gas mixture fed to the
461 photobioreactor. The continuous supply of O₂ also impacted the abundance of
462 microalgae in the culture, promoting the growth of aerobic heterotrophic bacteria.
463 Removing organic carbon from the synthetic wastewater and keeping CO₂ as a carbon

464 source in anaerobic conditions did not change the microbial distribution in the
465 reactor. The removal efficiency of NH_4^+ did not change a lot (26.6% versus 23.7%)
466 with the absence of organic carbon from phase II to phase III. In comparison, the
467 removal efficiency of PO_4^{3-} increased from 11.9% to 27.1%, and the removal
468 efficiency of CO_2 increased from 2.8% to 5.4%. The photobioreactor did not achieve
469 a net CO_2 removal regardless of the experimental conditions tested. A potential
470 strategy to increase CO_2 removal can be an intermittent CO_2 supply in the anaerobic
471 condition during the dark phase without organic carbon. As for the granulation
472 performance, high EPS production was observed, indicating the biomass had the
473 potential to form granules. However, no mature granules formed in the reactor,
474 potentially because of the lack of organic carbon in phase III and the lack of settling
475 time during the whole experiment. Therefore, the operational strategies tested in phase
476 II and phase III in this study could be used to quickly develop PNSB cultures from
477 activated sludge.

478 For long-term reactor performance, a higher HRT is recommended in the
479 earlier stage to ensure nutrient and COD removal performance. A longer light phase
480 might be helpful for PNSB growth. After the biomass is enriched to a proper
481 concentration, the loading could be increased step by step by reducing HRT. A settling
482 period or other operational conditions could be developed depending on specific
483 research goals, including specific wastewater treatment processes, bioproducts
484 production, and biomass utilization. In this study, each condition was operated for a
485 short period to establish PNSB communities. Further research should assess the
486 impact of various operational factors, such as light conditions, concentrations of CO_2
487 source, and the influent quality. Additionally, the long-term operation of the system
488 and its stability, as well as the enzymes involved in the metabolism pathways under

489 different conditions, should be thoroughly investigated.

490

491 **Acknowledgment**

492 This work was funded by the U.S. National Science Foundation under grant #2105726.

493 Any opinions, findings, and conclusions or recommendations expressed in this material

494 are those of the authors and do not necessarily reflect the views of the National Science

495 Foundation. The technical support from Dr. Gratia Deii Flores Salgado is gratefully

496 acknowledged.

497

498

499

500

501

502

503

504

505

506

507

508

509

510

511

512

513

514 **References**

515 [1] I. C. Vasilachi, D. M. Asiminicesei, D. I. Fertu, and M. Gavrilescu, "Occurrence
516 and fate of emerging pollutants in water environment and options for their
517 removal," *Water*, vol. 13, no. 2, p. 181, 2021.

518 [2] T. W. Seow *et al.*, "Review on wastewater treatment technologies," *Int. J. Appl.*
519 *Environ. Sci.*, vol. 11, no. 1, pp. 111-126, 2016.

520 [3] D. M. George, A. S. Vincent, and H. R. Mackey, "An overview of anoxygenic
521 phototrophic bacteria and their applications in environmental biotechnology for
522 sustainable Resource recovery," *Biotechnology reports*, vol. 28, p. e00563,
523 2020.

524 [4] S. Chitapornpan, C. Chiemchaisri, W. Chiemchaisri, R. Honda, and K.
525 Yamamoto, "Organic carbon recovery and photosynthetic bacteria population
526 in an anaerobic membrane photo-bioreactor treating food processing
527 wastewater," *Bioresource technology*, vol. 141, pp. 65-74, 2013.

528 [5] J. Chen *et al.*, "Photosynthetic bacteria-based technology is a potential
529 alternative to meet sustainable wastewater treatment requirement?,"
530 *Environment international*, vol. 137, p. 105417, 2020.

531 [6] H. Lu, G. Zhang, S. He, R. Zhao, and D. Zhu, "Purple non-sulfur bacteria
532 technology: a promising and potential approach for wastewater treatment and
533 bioresources recovery," *World Journal of Microbiology and Biotechnology*, vol.
534 37, no. 9, p. 161, 2021.

535 [7] S. Shaikh, N. Rashid, G. McKay, and H. R. Mackey, "Photobioreactor Design
536 for Polyhydroxyalkanoate Production Using Anoxygenic Photoheterotrophs: A
537 Review," *Fermentation*, vol. 9, no. 8, p. 778, 2023.

538 [8] P. Prachanurak, C. Chiemchaisri, W. Chiemchaisri, and K. Yamamoto,
539 "Biomass production from fermented starch wastewater in photo-bioreactor
540 with internal overflow recirculation," *Bioresource technology*, vol. 165, pp.
541 129-136, 2014.

542 [9] H. Lu, M. Peng, G. Zhang, B. Li, and Y. Li, "Brewery wastewater treatment and
543 resource recovery through long term continuous-mode operation in pilot
544 photosynthetic bacteria-membrane bioreactor," *Science of the Total
545 Environment*, vol. 646, pp. 196-205, 2019.

546 [10] T. Hülsen, E. M. Barry, Y. Lu, D. Puyol, and D. J. Batstone, "Low temperature
547 treatment of domestic wastewater by purple phototrophic bacteria: Performance,
548 activity, and community," *Water research*, vol. 100, pp. 537-545, 2016.

549 [11] A. Alloul, M. Cerruti, D. Adamczyk, D. G. Weissbrodt, and S. E. Vlaeminck,
550 "Operational strategies to selectively produce purple bacteria for microbial
551 protein in raceway reactors," *Environmental Science & Technology*, vol. 55, no.
552 12, pp. 8278-8286, 2021.

553 [12] T. Hülsen, E. M. Barry, Y. Lu, D. Puyol, J. Keller, and D. J. Batstone, "Domestic
554 wastewater treatment with purple phototrophic bacteria using a novel
555 continuous photo anaerobic membrane bioreactor," *Water research*, vol. 100,
556 pp. 486-495, 2016.

557 [13] A. Ghimire, G. Esposito, V. Luongo, F. Pirozzi, L. Frunzo, and P. N. Lens,
558 "Engineering Strategies for Enhancing Photofermentative Biohydrogen
559 Production by Purple Nonsulfur Bacteria Using Dark Fermentation Effluents,"
560 in *Microbial Fuels*: CRC Press, 2017, pp. 275-314.

561 [14] Y. Okubo and A. Hiraishi, "Population dynamics and acetate utilization kinetics
562 of two different species of phototrophic purple nonsulfur bacteria in a

563 continuous co-culture system," *Microbes and environments*, vol. 22, no. 1, pp.
564 82-87, 2007.

565 [15] J. Kaewsuk, W. Thorasampan, M. Thanuttamavong, and G. T. Seo, "Kinetic
566 development and evaluation of membrane sequencing batch reactor (MSBR)
567 with mixed cultures photosynthetic bacteria for dairy wastewater treatment,"
568 *Journal of Environmental Management*, vol. 91, no. 5, pp. 1161-1168, 2010.

569 [16] N. Rashid, M. N. Abdelnabi, A. S. Vincent, and H. R. Mackey, "Simultaneous
570 treatment of fruit juice industry wastewater and single-cell protein synthesis
571 using purple non-sulfur bacteria," *Biomass Conversion and Biorefinery*, vol. 13,
572 no. 18, pp. 16321-16332, 2023.

573 [17] B. S. Ross, "The effect of light intensity and reactor configuration on
574 *Rhodopseudomonas palustris* growth and hydrogen production," *Unpublished
575 Master's Thesis*, 2024.

576 [18] M. Cerruti, B. Stevens, S. Ebrahimi, A. Alloul, S. E. Vlaeminck, and D. G.
577 Weissbrodt, "Enrichment and aggregation of purple non-sulfur bacteria in a
578 mixed-culture sequencing-batch photobioreactor for biological nutrient removal
579 from wastewater," *Frontiers in bioengineering and biotechnology*, vol. 8, p.
580 557234, 2020.

581 [19] A. Alloul, S. Wuyts, S. Lebeer, and S. E. Vlaeminck, "Volatile fatty acids
582 impacting phototrophic growth kinetics of purple bacteria: paving the way for
583 protein production on fermented wastewater," *Water research*, vol. 152, pp.
584 138-147, 2019.

585 [20] S. Shaikh, N. Rashid, G. McKay, A. Liberski, and H. Mackey, "Nitrogen
586 influence on suspended vs biofilm growth and resource recovery potential of
587 purple non-sulfur bacteria treating fuel synthesis wastewater," *Biochemical
588 Engineering Journal*, vol. 190, p. 108754, 2023.

589 [21] M. Nuramkhaan *et al.*, "Isolation of microalgal strain from algal-bacterial
590 aerobic granular sludge and examination on its contribution to granulation
591 process during wastewater treatment in respect of nutrients removal, auto-
592 aggregation capability and EPS excretion," *Bioresource Technology Reports*,
593 vol. 8, p. 100330, 2019.

594 [22] B.-M. Wilén, R. Liébana, F. Persson, O. Modin, and M. Hermansson, "The
595 mechanisms of granulation of activated sludge in wastewater treatment, its
596 optimization, and impact on effluent quality," *Applied microbiology and
597 biotechnology*, vol. 102, pp. 5005-5020, 2018.

598 [23] N. Blansaer, A. Alloul, W. Verstraete, S. E. Vlaeminck, and B. F. Smets,
599 "Aggregation of purple bacteria in an upflow photobioreactor to facilitate
600 solid/liquid separation: impact of organic loading rate, hydraulic retention time
601 and water composition," *Bioresource Technology*, vol. 348, p. 126806, 2022.

602 [24] A. García *et al.*, "Wastewater treatment potential, light penetration profile and
603 biomass settling performance of a photo-sequencing batch reactor," *Journal of
604 Chemical Technology & Biotechnology*, vol. 98, no. 2, pp. 346-356, 2023.

605 [25] K. G. Coronado-Apodaca, M. Vital-Jácome, G. Buitrón, and G. Quijano, "A
606 step-forward in the characterization of microalgal consortia: microbiological
607 and kinetic aspects," *Biochemical Engineering Journal*, vol. 145, pp. 170-176,
608 2019.

609 [26] E. I. Valenzuela, J. A. Contreras, and G. Quijano, "Fast development of
610 microbial cultures for the anaerobic oxidation of CH₄ coupled to denitrification
611 employing widely available inocula," *Biochemical Engineering Journal*, vol.
612 184, p. 108492, 2022.

613 [27] E. Rice, R. Baird, A. Eaton, and S. Lenore, "Standard methods: For the
614 examination water and wastewater, 22nd edn. American Public Health
615 Association, American Water Works Association, Water Environmental
616 Federation," ed: ISSN, 2012.

617 [28] C. Osório *et al.*, "Pigments content (chlorophylls, fucoxanthin and
618 phycobiliproteins) of different commercial dried algae," *Separations*, vol. 7, no.
619 2, p. 33, 2020.

620 [29] X. Y. Li and S. F. Yang, "Influence of loosely bound extracellular polymeric
621 substances (EPS) on the flocculation, sedimentation and dewaterability of
622 activated sludge," *Water research*, vol. 41, no. 5, pp. 1022-1030, 2007.

623 [30] M. DuBois, K. A. Gilles, J. K. Hamilton, P. t. Rebers, and F. Smith,
624 "Colorimetric method for determination of sugars and related substances,"
625 *Analytical chemistry*, vol. 28, no. 3, pp. 350-356, 1956.

626 [31] O. Classics Lowry, N. Rosebrough, A. Farr, and R. Randall, "Protein
627 measurement with the Folin phenol reagent," *J biol Chem*, vol. 193, no. 1, pp.
628 265-75, 1951.

629 [32] J. San Martín, D. Puyol, Y. Segura, J. A. Melero, and F. Martínez, "A novel
630 photoanaerobic process as a feasible alternative to the traditional aerobic
631 treatment of refinery wastewater," *Journal of Water Process Engineering*, vol.
632 51, p. 103352, 2023.

633 [33] E. Madukasi, X. Dai, C. He, and J. Zhou, "Potentials of phototrophic bacteria in
634 treating pharmaceutical wastewater," *International Journal of Environmental
635 Science & Technology*, vol. 7, pp. 165-174, 2010.

636 [34] S. Liu, G. Zhang, J. Zhang, X. Li, and J. Li, "Performance, carotenoids yield
637 and microbial population dynamics in a photobioreactor system treating acidic
638 wastewater: Effect of hydraulic retention time (HRT) and organic loading rate
639 (OLR)," *Bioresource Technology*, vol. 200, pp. 245-252, 2016.

640 [35] A. S. Afifah, I. W. K. Suryawan, and A. Sarwono, "Microalgae production using
641 photo-bioreactor with intermittent aeration for municipal wastewater substrate
642 and nutrient removal," *Communications in Science and Technology*, vol. 5, no.
643 2, pp. 107-111, 2020.

644 [36] Y. Sun, Y. Sun, and X. Li, "Removal of pollutants and accumulation of high-
645 value cell inclusions in a batch reactor containing *Rhodopseudomonas* for
646 treating real heavy oil refinery wastewater," *Journal of Environmental
647 Management*, vol. 345, p. 118834, 2023.

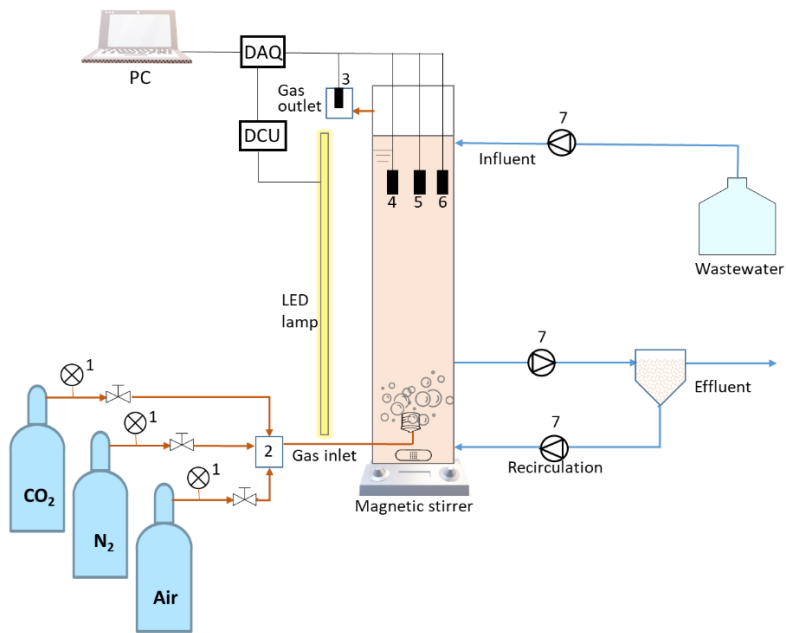
648 [37] Z. Dhaouefi, A. Toledo-Cervantes, K. Ghedira, L. Chekir-Ghedira, and R.
649 Muñoz, "Decolorization and phytotoxicity reduction in an innovative
650 anaerobic/aerobic photobioreactor treating textile wastewater," *Chemosphere*,
651 vol. 234, pp. 356-364, 2019.

652 [38] E. Jacob-Lopes, C. H. G. Scoparo, L. M. C. F. Lacerda, and T. T. Franco, "Effect
653 of light cycles (night/day) on CO₂ fixation and biomass production by
654 microalgae in photobioreactors," *Chemical Engineering and Processing: Process
655 Intensification*, vol. 48, no. 1, pp. 306-310, 2009.

656 [39] H. V. de Mendonça, J. P. H. B. Ometto, M. H. Otenio, I. P. R. Marques, and A.
657 J. D. Dos Reis, "Microalgae-mediated bioremediation and valorization of cattle
658 wastewater previously digested in a hybrid anaerobic reactor using a
659 photobioreactor: comparison between batch and continuous operation," *Science
660 of the Total Environment*, vol. 633, pp. 1-11, 2018.

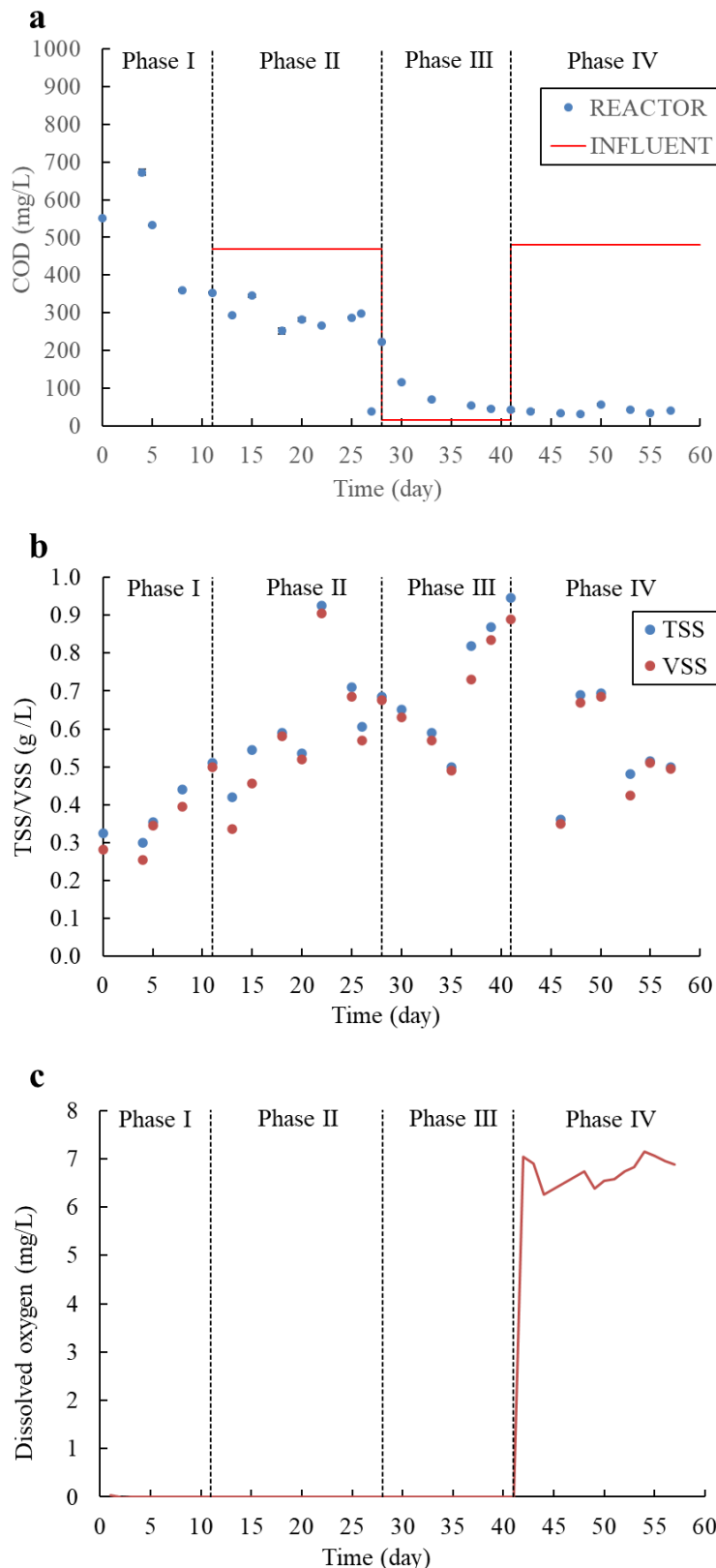
661 [40] F. Almomani *et al.*, "Impact of CO₂ concentration and ambient conditions on
662 microalgal growth and nutrient removal from wastewater by a photobioreactor,"

663 *Science of The Total Environment*, vol. 662, pp. 662-671, 2019.
664 [41] B. J. Reger and R. W. Krauss, "The photosynthetic response to a shift in the
665 chlorophyll a to chlorophyll b ratio of Chlorella," *Plant Physiology*, vol. 46, no.
666 4, pp. 568-575, 1970.
667 [42] F. Rezvani and M.-H. Sarrafzadeh, "Basic principles and effective parameters
668 for microalgae-bacteria granulation in wastewater treatment: a mini review,"
669 *International Journal of Environmental Science and Technology*, pp. 1-14, 2023.
670 [43] O. Y. Costa, J. M. Raaijmakers, and E. E. Kuramae, "Microbial extracellular
671 polymeric substances: ecological function and impact on soil aggregation,"
672 *Frontiers in microbiology*, vol. 9, p. 1636, 2018.
673 [44] E. Evans, M. R. Brown, and P. Gilbert, "Iron chelator, exopolysaccharide and
674 protease production in *Staphylococcus epidermidis*: a comparative study of the
675 effects of specific growth rate in biofilm and planktonic culture," *Microbiology*,
676 vol. 140, no. 1, pp. 153-157, 1994.
677 [45] R. J. De Vela, "A review of the factors affecting the performance of anaerobic
678 membrane bioreactor and strategies to control membrane fouling," *Reviews in
679 Environmental Science and Bio/Technology*, vol. 20, no. 3, pp. 607-644, 2021.
680 [46] G. Peng, F. Ye, and Y. Li, "Investigation of extracellular polymer substances
681 (EPS) and physicochemical properties of activated sludge from different
682 municipal and industrial wastewater treatment plants," *Environmental
683 technology*, vol. 33, no. 8, pp. 857-863, 2012.
684 [47] B.-M. Wilén, B. Jin, and P. Lant, "The influence of key chemical constituents
685 in activated sludge on surface and flocculating properties," *Water research*, vol.
686 37, no. 9, pp. 2127-2139, 2003.
687 [48] S. Stegman, D. J. Batstone, R. Rozendal, P. D. Jensen, and T. Hülsen, "Purple
688 phototrophic bacteria granules under high and low upflow velocities," *Water
689 Research*, vol. 190, p. 116760, 2021.
690 [49] M. Custodio, R. Peñaloza, C. Espinoza, W. Espinoza, and J. Mezarina,
691 "Treatment of dairy industry wastewater using bacterial biomass isolated from
692 eutrophic lake sediments for the production of agricultural water," *Bioresource
693 Technology Reports*, vol. 17, p. 100891, 2022.
694 [50] D. Zhang, W. Li, X. Huang, W. Qin, and M. Liu, "Removal of ammonium in
695 surface water at low temperature by a newly isolated *Microbacterium* sp. strain
696 SFA13," *Bioresource technology*, vol. 137, pp. 147-152, 2013.
697 [51] S. N. A. Azaman, N. Nagao, F. M. Yusoff, S. W. Tan, and S. K. Yeap, "A
698 comparison of the morphological and biochemical characteristics of *Chlorella
699 sorokiniana* and *Chlorella zofingiensis* cultured under photoautotrophic and
700 mixotrophic conditions," *PeerJ*, vol. 5, p. e3473, 2017.
701 [52] N. B. Chowdhury, A. Alsiyabi, and R. Saha, "Characterizing the interplay of
702 rubisco and nitrogenase enzymes in anaerobic-photoheterotrophically grown
703 *Rhodopseudomonas palustris* CGA009 through a genome-scale metabolic and
704 expression model," *Microbiology Spectrum*, vol. 10, no. 4, pp. e01463-22, 2022.
705 [53] M. T. Madigan and D. O. Jung, "An overview of purple bacteria: systematics,
706 physiology, and habitats," *The purple phototrophic bacteria*, pp. 1-15, 2009.
707 [54] S. Romagnoli and F. R. Tabita, "Carbon dioxide metabolism and its regulation
708 in nonsulfur purple photosynthetic bacteria," in *The purple phototrophic
709 bacteria*: Springer, 2009, pp. 563-576.
710 [55] H. Lu, G. Zhang, T. Wan, and Y. Lu, "Influences of light and oxygen conditions
711 on photosynthetic bacteria macromolecule degradation: different metabolic
712 pathways," *Bioresource technology*, vol. 102, no. 20, pp. 9503-9508, 2011.



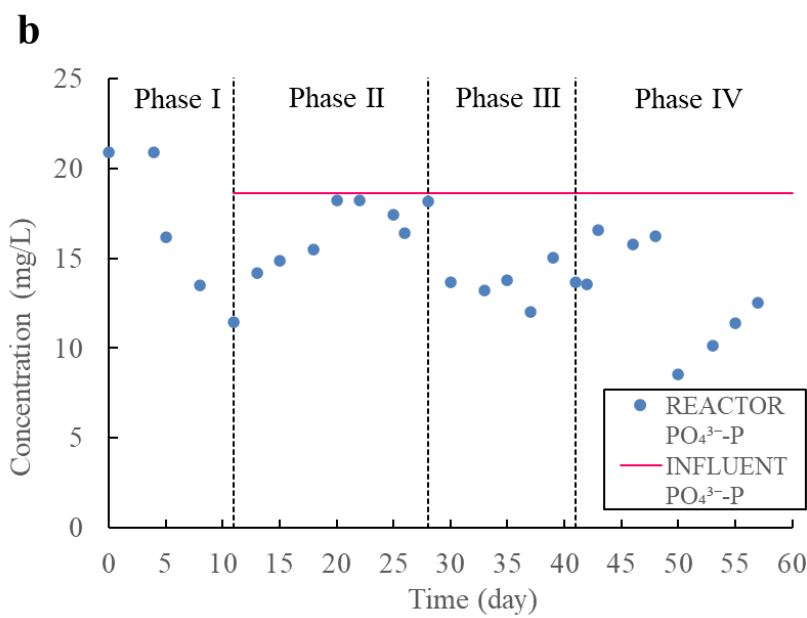
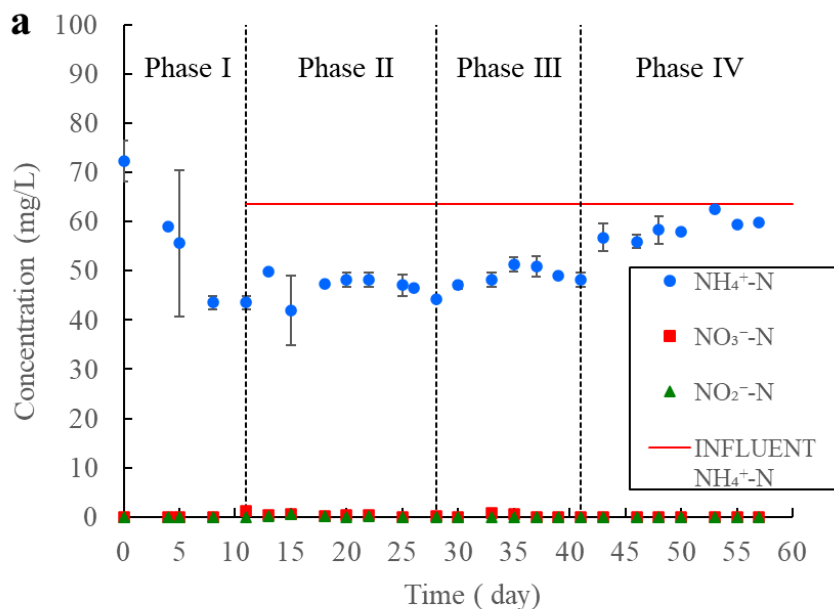
713

714 **Figure 1.** Schematic representation of the experimental setup. DAQ and DCU stand
 715 for data acquisition card and digital control unit, respectively; (1) mass flow
 716 controller, (2) gas mixing chamber, (3) CO₂ gas sensor, (4) pH sensor, (5) DO sensor,
 717 (6) temperature sensor, (7) peristaltic pump



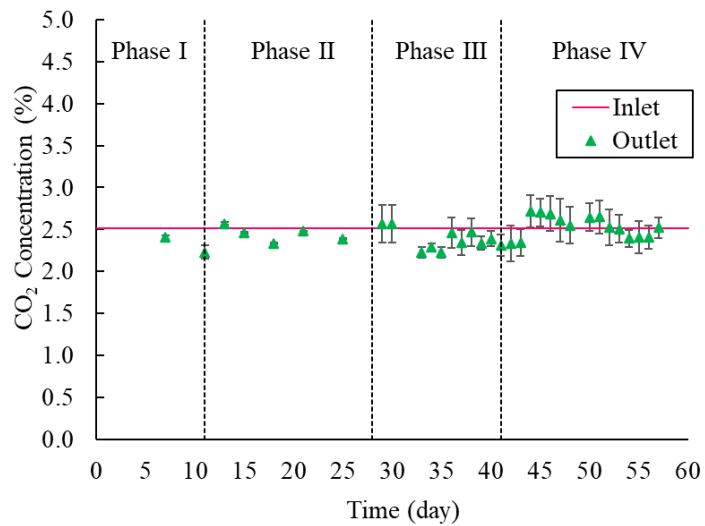
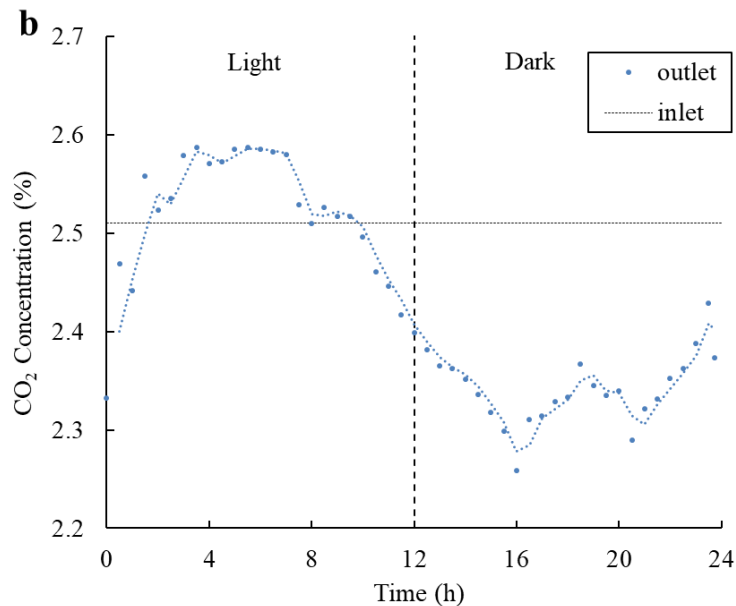
718

719 **Figure 2.** Time course of (a) COD, (b) TSS and VSS, and (c) dissolved oxygen
720 concentrations in the four experimental phases tested in the photobioreactor



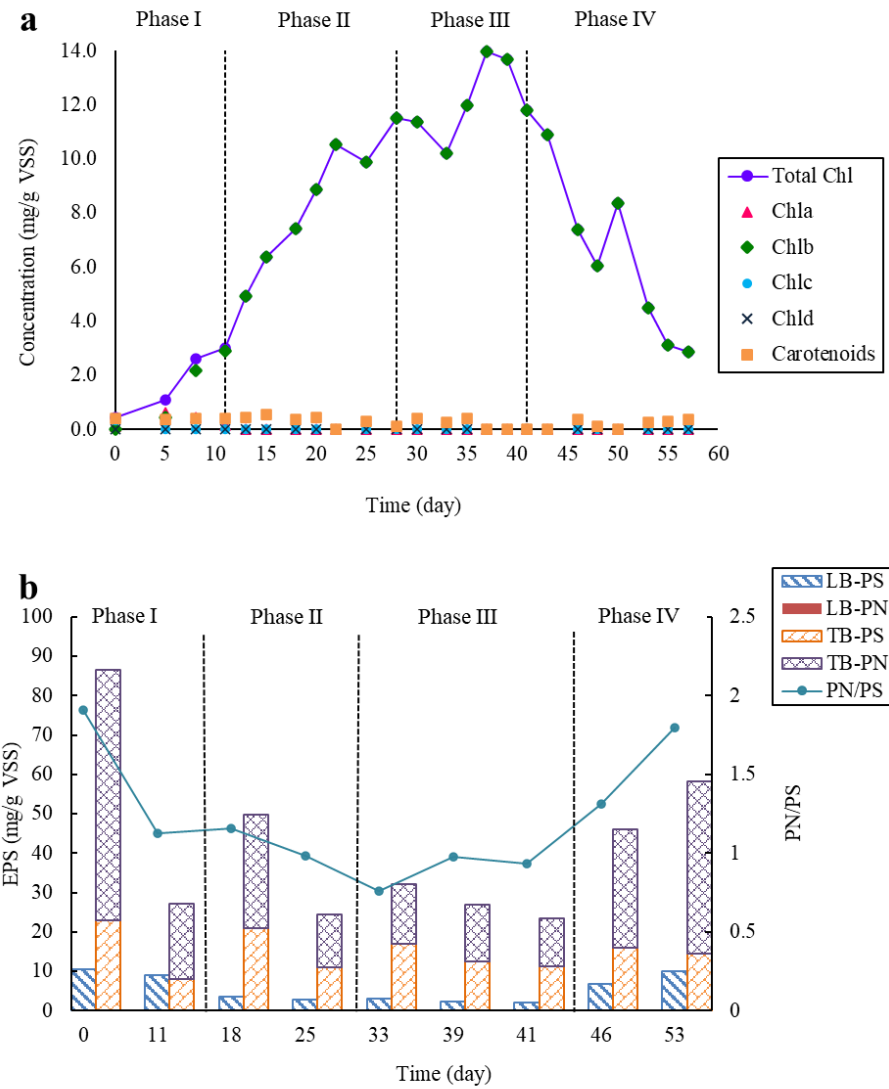
721

722 **Figure 3.** Time course of (a) inorganic nitrogen species, and (b) PO_4^{3-} -P concentration
723 in the experimental phases tested in the photobioreactor

a**b**

724

725 **Figure 4.** (a) Time course of CO_2 concentration in gas phase in the experimental phases
726 tested in the photobioreactor; (b) One-day dynamics of the CO_2 concentration of
727 experimental phase III (average)



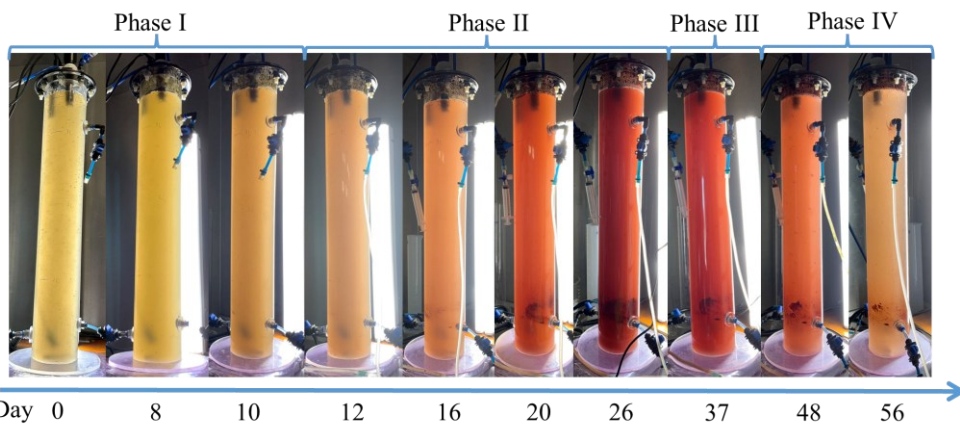
728

729 **Figure 5.** Biomass content of (a) chlorophyll and carotenoids, as well as (b) EPS
730 determined in the experimental phases tested

731

732

733



734

735 **Figure 6.** Color changes of the bioreactor in each experimental phase

736

737

738

739

740

741

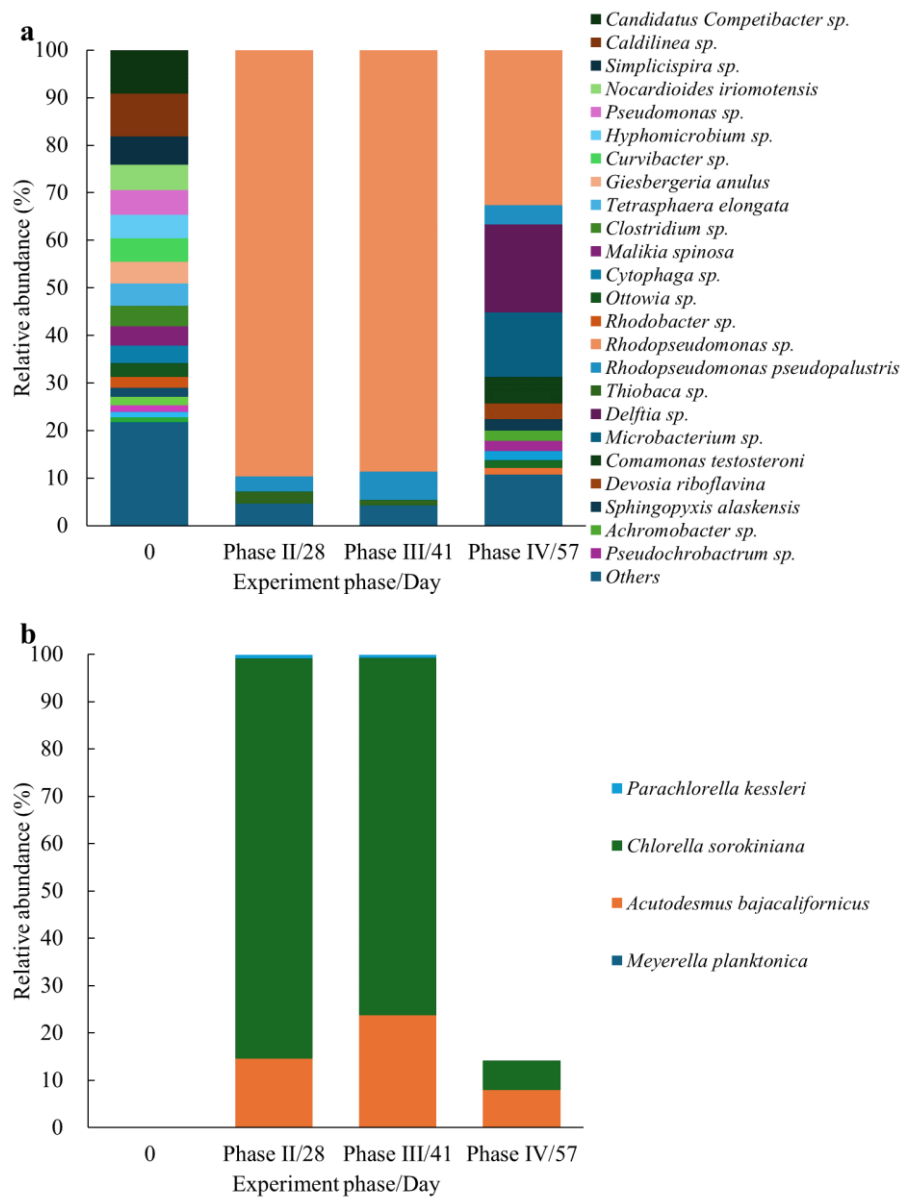
742

743

744

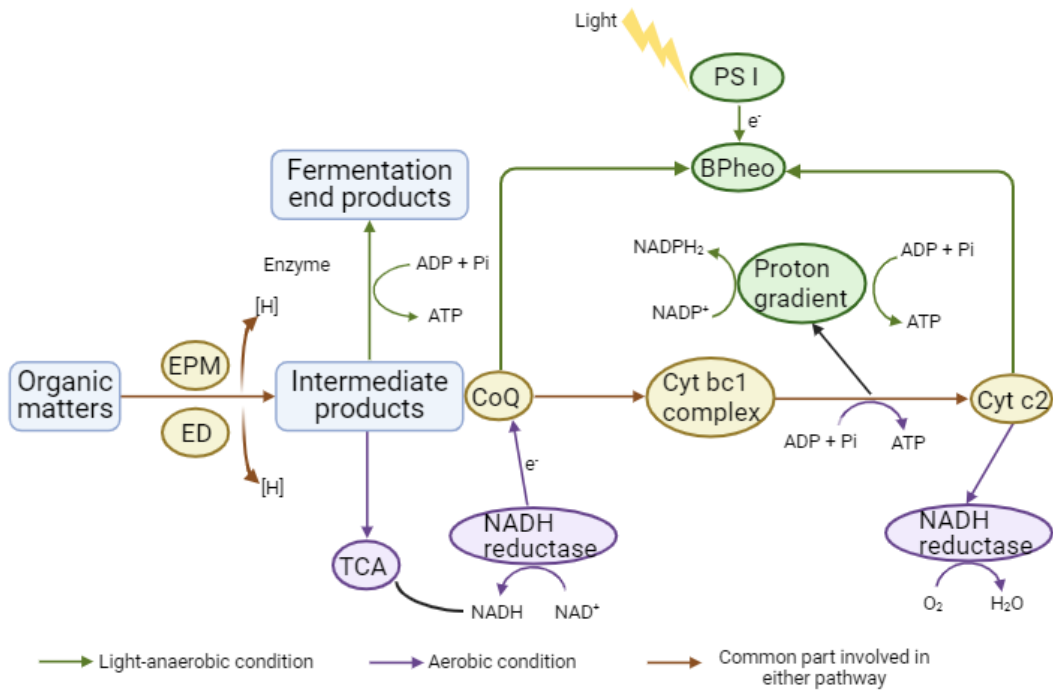
745

746



747

748 **Figure 7.** Microbial community composition at the species level as determined by (a)
749 16S RNA sequencing of biomass; (b) 18S RNA sequencing of biomass (microalgae)



750

751 **Figure 8.** Mechanisms of COD removal in the bioreactor in each condition. Figure
752 was adapted from Lu et al. [55].

753

754

755

756

757

758

759

760

761 **Table 1.** Influent COD concentration and composition of the gas fed in each
 762 experimental phase.

Experimental phase	Days	HRT (day)	Influent COD (mg/L)	O₂ in gas phase (%)	CO₂ in gas phase (%)	N₂ in gas phase (%)
I	0-11	Batch for liquid phase	469.3±10.3	0	2.5	97.5
II	12-28	2.5	469.3±10.3	0	2.5	97.5
III	29-41	2.5	16±2.8	0	2.5	97.5
IV	42-57	2.5	479.7±10.0	20.4	2.5	76.0

763

764 **Table 2.** Average COD, N, and P removal performance achieved in each experimental phase.

Experimental phase	COD			NH ₄ ⁺ -N			PO ₄ ³⁻ -P			Removal ratio COD:N:P	Biomass specific growth rate (day ⁻¹)
	Removal efficiency (%)	Removal rate (g COD/(m ³ ·d))	Specific removal rate (g COD/(kg VSS·d))	Removal efficiency (%)	Removal rate (g N/(m ³ ·d))	Specific removal rate (g N/(kg VSS·d))	Removal efficiency (%)	Removal rate (g P/(m ³ ·d))	Specific removal rate (g P/(kg VSS·d))		
I	35.9	18	56.4	39.8	2.62	8.2	20.4	0.9	2.7	100:15:5	0.06
II	36.7±7.5	68.8±15.3	128.7±42.9	26.6±4.4	6.8±1.1	12.9±4.3	11.9±13.2	1.2±1.0	2.5±2.3	100:10:2	0.10
III	NA ^a	NA ^a	NA ^a	23.7±4.1	6.0±1.0	9.4±2.0	27.1±11.4	1.7±0.9	2.7±1.5	-	0.09
IV	91.7±1.6	175.8±3.2	311.8±116.9	10.0±6.7	2.4±1.7	3.9±2.5	29.9±15	2.2±1.2	4.0±2.5	100:1:1	0.07

765 a. NA: COD was not supplied in this experimental phase.

766

767

768

769

770 **Table 3.** Suggested PNSB metabolic pathway in each experimental phase based on the
 771 CO₂ and COD metabolism recorded in the present work.

Experimental phase	Carbon source	Condition of O₂	Main metabolic pathway	
			Light	Dark
II	Organic carbon & CO ₂	Anaerobic	Photoheterotrophic	Fermentation/anaerobic respiration
III	Sole CO ₂	Anaerobic	Photoautotrophic	Reductive tricarboxylic acid (rTCA) cycle
IV	Organic carbon & CO ₂	Aerobic	Aerobic respiration	Aerobic respiration

772